IJMOT

INTERNATIONAL JOURNAL OF MICROWAVE AND OPTICAL TECHNOLOGY

VOL. 3, NO. 3, JULY 2008

Nonlinear Distortion Generation Mechanisms in Wireless Polar Transmitters

Pedro M. Cabral*, José C. Pedro* and José A. Garcia**

*Instituto de Telecomunicações – Universidade de Aveiro
Campus Universitário de Santiago, 3810-193 Aveiro, Portugal
Tel: +351 234377900; Fax: +351 234377901; E-mail: pcabral@ua.pt

**Departamento Ingeniería de Comunicaciones
Universidad de Cantabria, 39005, Santander, SPAIN
Tel: +34 942 200887; Fax: +34 942 201488; E-mail: joseangel.garcia@unican.es

***Abstract*- This paper discusses the most important nonlinear distortion generation mechanisms present in modern wireless polar transmitters. It begins by using the spectrum and power efficiency trade-off in wireless communication systems to justify the polar transmitter architecture. Then, it identifies the key fidelity impairments under a traditional two-tone excitation, and uses an analytical formulation of its nonlinearities to illustrate the distortion levels that should be expected from such a system.**

***Index Terms*- Efficiency, nonlinear distortion, polar transmitters, power amplifiers.**

I. INTRODUCTION

Nowadays, wireless telecommunication links are dominated by the trade-off between spectral and supply power efficiency. This requires amplitude and phase modulation formats to code the source symbols. In a traditional Cartesian transmitter (Tx) chain, in-phase and quadrature versions of one Radio Frequency (RF) carrier are simultaneously modulated with the appropriate real and imaginary components of the low-pass equivalent modulating envelope, in an I/Q modulator.

Afterwards, these are combined to generate the desired amplitude (AM) and phase modulation (PM) format, which is finally processed by a supposedly linear RF power amplifier (PA).

In such a Tx architecture, each of the RF blocks has to process an amplitude and phase modulated carrier. So, the Cartesian architecture has an important drawback in power supply efficiency because high fidelity of amplitude modulation formats require highly linear, but, unfortunately, inefficient, class-A or -AB PAs.

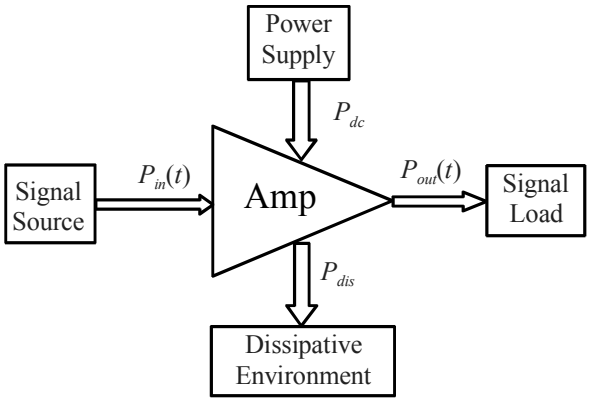

Fig. 1. Conceptual diagram of a PA for studying its associated power relations.

Indeed, if we consider the PA shown in Fig. 1, where $P_{in}(t)$ and $P_{out}(t)$ are the instantaneous input and output signal powers, P_{dc} is the dc supplied power and P_{dis} is the dissipated power (in any form like heat or harmonic distortion), the energy conservation principle determines that:

$$P_{dc} + P_{in} = P_{out} + P_{dis} \quad (1)$$

So, the PA gain, will have to be given by

$$G = \frac{P_{out}}{P_{in}} = 1 + \frac{P_{dc} - P_{dis}}{P_{in}} \quad (2)$$

while the power added efficiency (*PAE*), must be

$$PAE = \frac{P_{out} - P_{in}}{P_{dc}} = 1 - \frac{P_{dis}}{P_{dc}} \quad (3)$$

These two expressions, (2) and (3), clearly indicate that a good compromise between linearity [constant gain independent of $P_{in}(t)$] and *PAE*, can only be achieved by a very small dissipated power, Pdis→0, and a dc power supplied to the PA that is proportional to $P_{in}(t)$. That is, if the instantaneous input power $P_{in}(t)$ varies with time, due to the amplitude modulation, then the $P_{dc}(t)$ should track that variation.

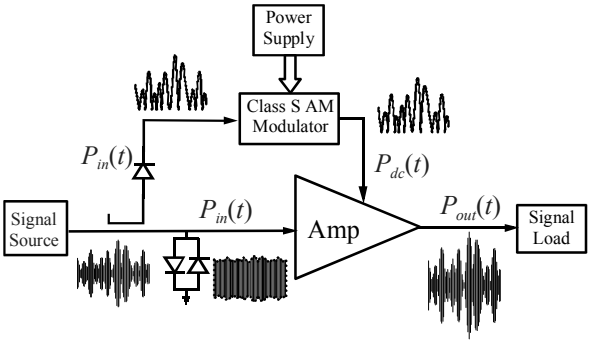

Fig. 2. Conceptual PA diagram embedded in an envelope elimination and restoration scheme.

This is the concept depicted in Fig. 2, which describes the so-called envelope elimination and restoration (EER), or Kahn [1], method. In that scheme, the envelope is first eliminated by a limiter, to guarantee that the amplifier is always driven into saturation, and then restored by the dc power modulator (represented by a highly efficient Class-S switching-mode power supply). This EER technique led to the polar Tx, see Fig. 3, in which the amplitude and phase signals are independently treated until the last stage, the RF PA. Thus, for efficiency reasons, this must be a switching device, operating in a highly efficient class-E or F mode. Similarly to the EER, the PA excitation is a constant envelope modulated carrier, while the amplitude is dynamically restored through its supply voltage.

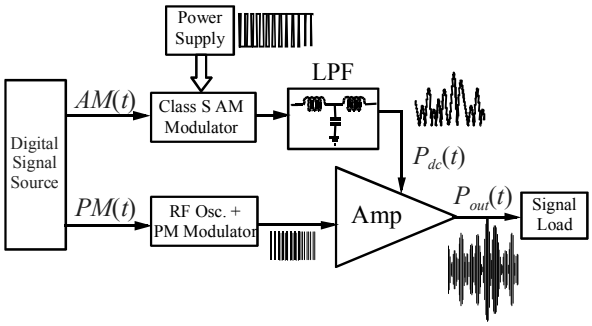

Fig. 3. Conceptual PA diagram embedded in an polar architecture scheme.

In theory, such a Tx architecture would be 100% efficient and ideally linear. In practice, however, it can be shown that its efficiency is approximately given by the product of the power supply modulator and PA efficiencies. On the other hand, its linearity is impaired by a series of nonlinear phenomena. These will be the focus of the rest of this paper.

II. LINEARITY IMPAIRMENTS

The studied architecture is based on a conceptual system level transmitter description, shown in Fig. 4.

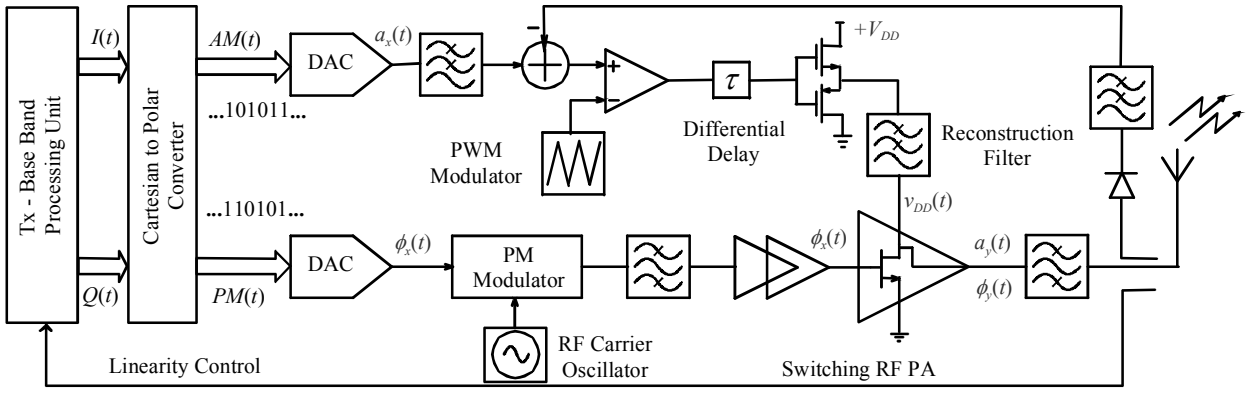

Fig. 4. System model of a wireless Tx with polar architecture.

The nonlinear impairment mechanisms considered [2-5], were:

(i) Finite AM modulator bandwidth;
(ii) Differential delay between the amplitude signal and the phase modulated carrier;
(iii) RF switching PA nonlinear transfer function [$v_{DD}(t)$-to-$a_y(t)$ conversion, [6], and carrier feed-through].

A. Finite Bandwidth and Differential Delay

The finite AM modulator bandwidth is represented, in Fig. 4, by a low-pass reconstruction filter, $F(\omega)$. This filter is responsible for eliminating all the modulation replicas, centered at the harmonics of ω_s, the Class-S modulator clock (or sampling) frequency. Unfortunately, in a real application scenario, $F(\omega)$ will not be an ideal brick-wall filter and will thus introduce amplitude and phase distortions in the $a_x(t)$-to-$v_{DD}(t)$ conversion.

Besides that, since the AM and PM signals travel through two different paths, there will be an unavoidable differential delay (τ) between them. Thus, the reconstructed analogue amplitude signal, the supply voltage of the RF PA, will be of the form: $v_{DD}(t) = a_x(t-\tau)$.

The analytical model for these two nonlinear impairments was initially presented in [2] and then analyzed in more detail in [5]. There, it was shown that, although these causes are linear processes, their impact on the Tx output is a source of nonlinear distortion.

B. Nonlinear $v_{DD}(t)$-to-$a_y(t)$ Conversion and Carrier Feed-Through

While the filter bandwidth and differential delay could be attributed to the particular polar Tx architecture, the $v_{DD}(t)$-to-$a_y(t)$ conversion and carrier feed-through were found to be due to the RF switching PA circuit imperfections [5].

An illustrative example of these is depicted in Fig. 5. In fact, this figure presents the measured $a_y(v_{DD})$ function of a pHEMT based Class-E PA. Note the non-zero a_y for vanishingly small v_{DD} and the subsequent nonlinear $a_y(v_{DD})$ relation encountered for higher v_{DD} values. The observed phenomenon, for the lowest end of v_{DD} operation, is due to the carrier feed-through (usually attributed to the RF carrier leakage via the input-output capacitance).

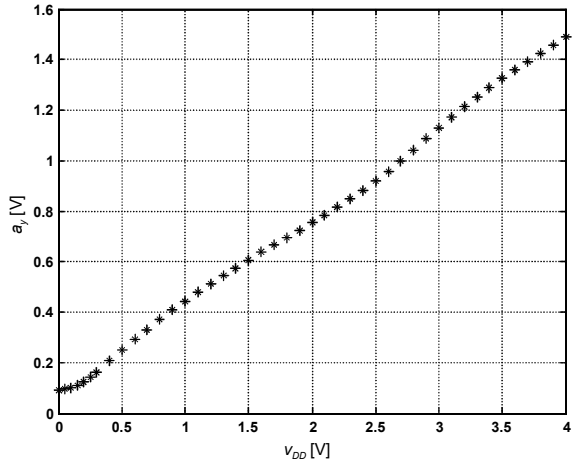

Fig. 5. $v_{DD}(t)$-to-$a_y(t)$ characteristic of a pHEMT based Class-E PA.

The nonlinearity appearing at the region of intermediate values of v_{DD} was found to be due to kinks of the pHEMT output I/V characteristics. Finally, the $a_y(v_{DD})$ nonlinearity, noticeable for the highest v_{DD} range, could be related to a parasitic current-mode operation of the (supposedly) switching-mode Class-E PA.

III. EXPERIMENTAL TESTS

As an illustration of these polar Tx linearity impairments, we picked up a switching mode PA circuit, a low-power pHEMT based class-E PA, and conducted several simulation and laboratory measurements on it. Fig. 6 shows a simplified schematic diagram of the tested switching mode PA.

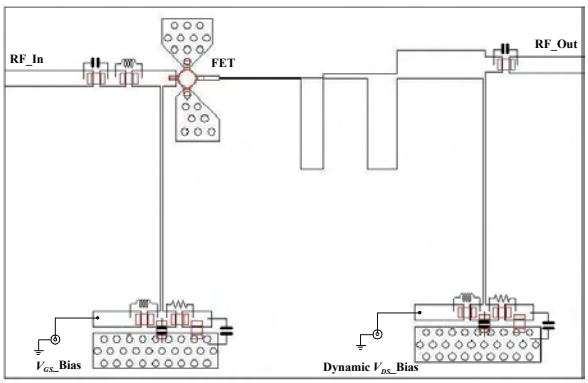

Fig. 6. Simplified circuit diagram of the class-E switching PA used in the experimental and simulated tests.

For the simulated tests the PA system-level model was inserted in a block diagram similar to the one presented in Fig. 3 and implemented in a commercial circuit level/system level co-simulation tool. The actual laboratory measurement setup used is presented in Fig. 7.

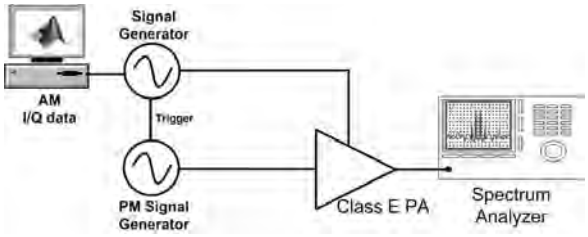

Fig. 7. Complete measurement setup used in the distortion characterization tests.

The two different situations previously presented in section II.A: finite AM modulator bandwidth and differential delay between the output amplitude signal and modulated carrier were herein respectively represented by a 3dB ripple third-order Chebyshev reconstruction filter and by a delay line, in the digital domain.

In both cases, the $v_{DD}(t)$-to-$a_y(t)$ nonlinearity was included to verify its zone of impact and relative importance.

Fig. 8 presents measured and simulated results of C/IMD3 and C/IMD5 for the finite AM modulator normalized bandwidth, Ω.

In this case, it is obvious that, for narrow-band filters, the C/IMD will be smaller than the obtained when the filter bandwidth is high enough to accommodate all the meaningful envelope components. Besides that, it is now clear that, for wide filter bandwidths, the distortion will be mainly due to the RF PA $v_{DD}(t)$-to-$a_y(t)$ nonlinearity.

The results were obtained considering a two-tone input signal centered at 900MHz with a tone separation of 100kHz.

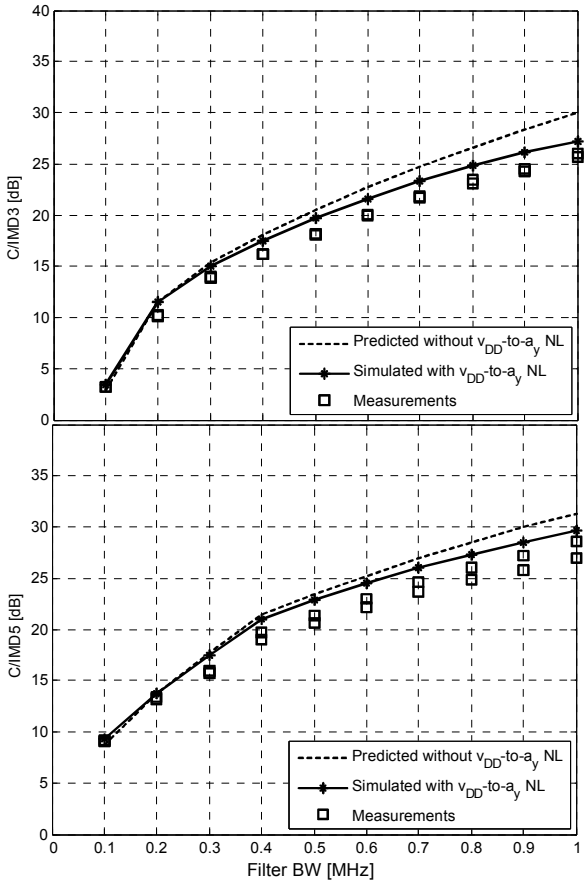

Fig. 8. C/IMD3 and C/IMD5 for $2<\Omega<20$.

The impact of the delay is depicted in the C/IMD3 and C/IMD5 measured and simulated results, shown in Fig. 6.

Looking into Fig. 9, it is now possible to see that, for small delay values, the distortion is due to the RF PA $v_{DD}(t)$-to-$a_y(t)$ nonlinearity. But, for highest delays, it can be completely described by the nonlinearity due to that delay mismatch.

IV. CONCLUSION

This paper presented a justification of the polar TX architecture and discussed its major sources of nonlinearity. Amplitude and phase signal delay mismatch, finite AM modulator bandwidth and AM restoration nonlinearity were used to illustrate the C/IMD3 and C/IMD5 levels that should be expected from current PA and AM modulator technologies.

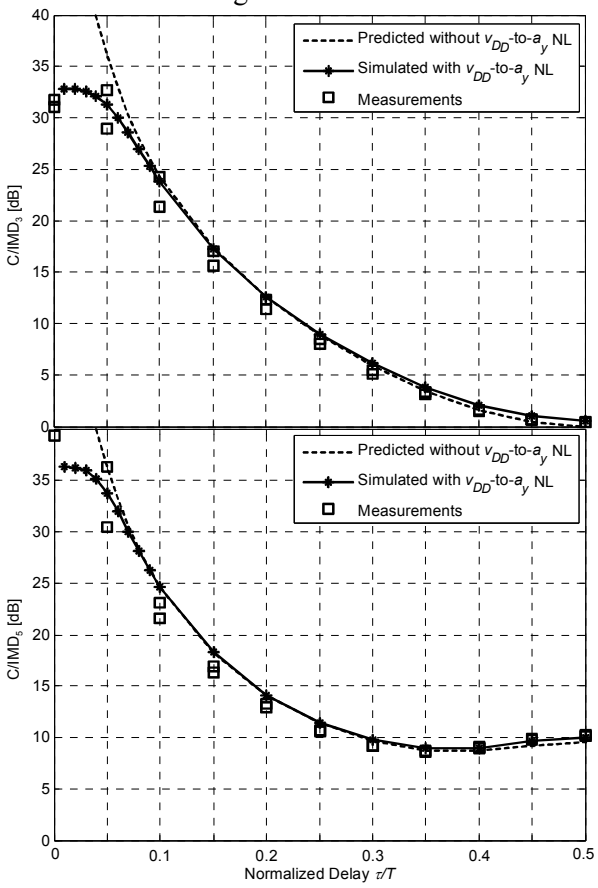

Fig. 9. C/IMD3 and C/IMD5 for $0<\tau/T<0.5$.

ACKNOWLEDGEMENT

The authors would like to thank the support provided by the EC, through TARGET NoE, IST-1-507893-NOE, and to MEC Project TEC2005-07985-C03-01.

REFERENCES

[1] L. R. Kahn, "Single-Sideband transmission by envelope elimination and restoration," *Proc. IRE*, vol. 40, no. 7, pp. 803-806, Jul. 1952.

[2] F. H. Raab, "Intermodulation distortion in Kahn-technique transmitters," *IEEE Trans. on MTT*, vol. 44, no. 12, pp. 2273-2278, Dec. 1996.

[3] D. Milosevic, J. van der Tang and A. van Roermund, "Intermodulation products in the EER technique" applied to class-E amplifiers," *Int.*

Symp. on Circuits and Syst. Dig., pp.637-640, Vancouver, May 2004.

[4] N. Wang, X. Peng, V. Yousefzadeh, D. Maksimovic´, S. Pajic´, and Z. Popovic´, "Linearity of X-Band class-E power amplifiers in EER operation," *IEEE Trans. on MTT*, vol. 53, no. 3, pp.1096-1102, Mar. 2005.

[5] José C. Pedro, José A. Garcia and Pedro M. Cabral, "Nonlinear Distortion Analysis of Polar Transmitters", *IEEE MTT-S Int. Microwave Symp. Dig.*, Honolulu, Hawaii, USA, pp. 957-960, Jun. 2007.

[6] M. Kazimierczuk, "Collector amplitude modulation of the class E tuned power amplifier," *IEEE Trans. on CAS*, vol. CAS-31, no. 6, pp.543-549, Jun. 1984.